Science of Sintering, **50** (2018) 29-38

doi: https://doi.org/10.2298/SOS1801029K

UDK 531.3; 622.785; 546.824

Effect of Chemical Composition on Microstructural Properties and Sintering Kinetics of $(Ba,Sr)TiO_3$ Powders

D. A. Kosanović[1*)], V. A. Blagojević[1], N. J. Labus[1], N. B. Tadić[2], V. B. Pavlović[1], M. M. Ristić[3]

[1]Institute of Technical Sciences of the Serbian Academy of Sciences and Arts, Knez Mihailova 35/IV, 11000 Belgrade, Serbia

[2]Faculty of Physics, University of Belgrade, Studentski Trg 12, 11000 Belgrade, Serbia

[3]Serbian Academy of Sciences and Arts, Knez Mihailova 35, 11000 Belgrade, Serbia

Abstract:

Barium strontium titanate powders with different Ba:Sr ratios were investigated to determine the influence of the initial composition of powder mixture on microstructural properties and sintering kinetics. It was determined that $BaCO_3$ and $SrCO_3$ react differently to mixing, resulting in $Ba_{0.5}Sr_{0.5}CO_3$ in the sample with 80% Ba and different contents of $Ba_{1-x}Sr_xTiO_3$ in samples with 50% and 20% Ba. In addition, the morphology is also different, with higher Sr content leading to larger particles size and less agglomeration. The different chemical content of the initial powder mixture also has a marked impact on the sintering process: the onset of sintering shifts towards higher temperature with higher Sr content, while the average apparent activation energy of sintering is the highest for the sample with 80% Ba and the lowest for the mixture with 50% Ba. In addition, hexagonal-to-cubic phase transformation was observed in parallel with the sintering process, where the position of the phase transition shifts to lower temperatures with an increase in Sr content. This is consistent with the behavior of low-temperature phase transitions of BST. The phase transition was not observed in sintered samples, suggesting that there is a size-dependence of the phase transition temperature.

Keywords: *Barium strontium titanate; Sintering kinetics; Phase transition; Size dependence.*

1. Introduction

Barium strontium titanate $(Ba,Sr)TiO_3$ (BST), a typical ferroelectric material with a tetragonal structure, belongs to the family of (ABO_3) perovskites, composed of titanate, barium titanate $(BaTiO_3)$ and strontium titanate $(SrTiO_3)$ [1-5].Pure barium titanate ceramic undergoes a para-ferroelectric phase transition at 120 ^oC from cubic to tetragonal phase, while the strontium titanate, which has para-ferroelectric phase transition at 163 ^oC, is usually added into barium titanate in order to lower the Curie point (Tc) and to increase the room temperature dielectric constant of the material [6]. BST ferroelectrics exhibit high dielectric permittivity and have been widely investigated both in films and ceramics.

BST thin films are promising materials for high-density dynamic random-access

*) **Corresponding author**: kosanovic.darko@gmail.com

memories (DRAMs) [7-9]. BST ceramics are considered good candidates for applications in phased array antennas [10], as well as in capacitors, sensors and PTC thermistors [11-13].Properties of BST ceramic are strongly dependent on the stoichiometry, homogeneity, particle size and phase purity of the BST powder [14-16], which in turn depends on the synthesis method used [17-20].The stoichiometry and structural characteristics, including the concentration of oxygen vacancies, of BST powder, is strongly influenced by the initial Ba/Sr ratio in precursor solution relative to Ti, as well as the type of precursor used in the reaction [21].

In general, BT and BST ceramics are prepared by the conventional mixed oxide method based on calcining the mixed oxide or carbonate powders. However, the calcined powders usually consist of chemically inhomogeneous particles with large grain sizes. This makes them unsuiTab. for use as raw material for advanced electronic components. Therefore, other wet chemical processes including co-precipitation, spray pyrolysis, oxalate, sol-gel and hydrothermal synthesis have been reported [22-28].

Barium and strontium react differently with titanium, where strontium atoms, compared to barium, are more readily incorporated into the BST structure [29]. At room temperature for the solid solution in ferroelectric phase, Ba content is in the range of 0.7 to 1.0, while the content of Ba in paraelectric phase is less than 0.7 [30]. In order to obtain homogeneous crystalline samples, a commonly used procedure is the sintering of BST powders at temperatures 1200-1350 ^{o}C [31, 32], although glass-ceramic BST powders can be sintered at as low as 1000 ^{o}C [33].

Herein we present a study of the influence of the chemical composition of BST powder on its microstructural properties and sintering kinetics, as a part of an a broader study of the influence of composition and microstructural parameters on sintering behavior and functional properties of BST [34-36].

2. Experimental procedure

For the synthesis of (Ba,Sr)TiO_3 (BST) system following commercially available $BaCO_3$ (99.8% Aldrich), $SrCO_3$ (99.8% Aldrich) and TiO_2 (99.99% Aldrich) powders were mixed and homogenized in three different ratios of Ba and Sr (80/20, 20/80 and 50/50).The powder mixtures were dried and calcined at a temperature of 800 ^{o}C, for 3 h inside a chamber furnace.

Compaction of powders was uniaxial double-sided, providing green bodies with a diameter of 8 mm on hydraulic press RING, P-14 (VEB THURINGER). Pellets were compacted under 392 MPa. They were treated nonisothermally in a dilatometer (BährGerätebau GmbH Type 802s) at a heating rate of 10, 15, and 20 °C/min up to 1300 °C, followed by isothermal holding at 1300 °C for 30 min.

The X-ray powder diffraction patterns were obtained using aRigakuUltima IV X-ray diffraction (XRD) instrument in thin film geometry with grazing incidence angle of 0.5°, using Ni-filtered CuKα radiation (λ = 1.54178 Å). Diffraction data were acquired over the scattering angle 2θ from 10° to 70° with a step of 0.05° and acquisition rate of 2°/min and obtained data were analyzed with PDXL 2 software. Rietveld analysis was performed with full refinement using GSAS II software package [37]. Obtained values of R_{wp} (weighted residual factor) varied from 11.0 % to 18.3 % and the Goodness of Fit indicator was GoF~1.

The microstructural characterization of the BST powders was performed by a Scanning Electron Microscope (SEM, JSM-6390 LV JEOL, 20 kV) coupled with EDS (Oxford Instruments X-MaxN). Before microstructure characterization, the samples were coated with gold in a sputter coater (SCD 005; BALTEC, Scotia, NY).

3. Results and Discussion

In order to investigate the influence of chemical composition on the state of pre-sintered samples with different ratios of Ba to Sr were examined using XRD. The patterns of different samples were used for Rietveld analysis to determine their phase composition (Tab. I) and microstructural parameters of selected phases (Tab. II). In samples with 50 and 80% Sr, formation of $Ba_xSr_{1-x}TiO_3$ phases, as the product of the chemical reaction between $BaCO_3$, $SrCO_3$ and TiO_2, is observed, while in the sample with 20% Sr, no chemical reaction is observed, although formation of mixed barium-strontium carbonate $Ba_{0.5}Sr_{0.5}CO_3$ is observed, in addition to pure $BaCO_3$ existence.Since $BaCO_3$ and $SrCO_3$ share the same aragonite crystal structure, they are known to form mixed carbonates [38]. The absence of $SrCO_3$ lines in XRD pattern suggests that mechanical homogenization of the initial powder produced $Ba_{0.5}Sr_{0.5}CO_3$ until Sr was exhausted, leaving an excess of $BaCO_3$ in the system. Further analysis has shown that the composition of $Ba_xSr_{1-x}TiO_3$ phases depends on the composition of the starting mixture and the ratio of Ba to Sr in $Ba_xSr_{1-x}TiO_3$ product generally corresponds to their ratio in the starting mixture.

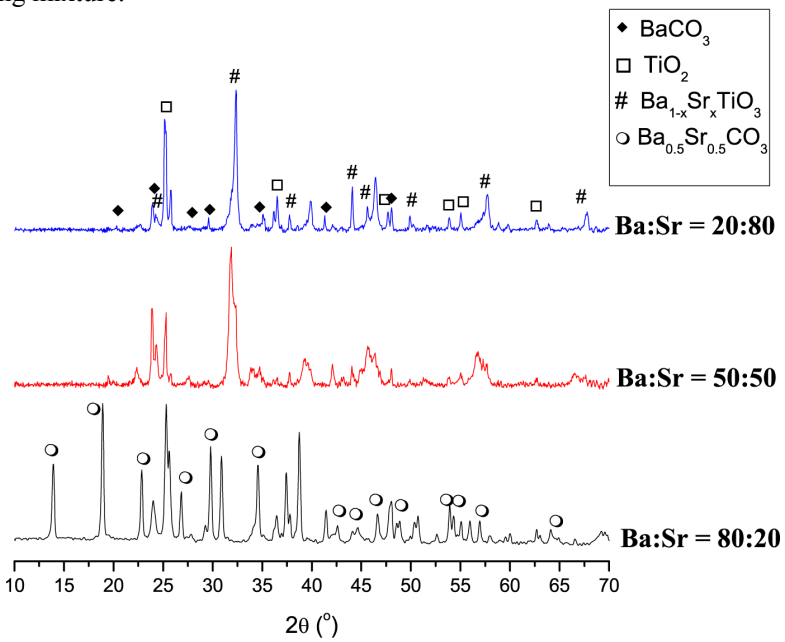

Fig. 1. XRD patterns of pre-sintered samples with different Ba-to-Sr ratios.

Tab.I Phase composition of pre-sintered samples.

Sample	TiO_2(wt%)	$BaCO_3$ (wt%)	$SrCO_3$ (wt%)	New phase (wt%)	
Ba80-Sr20 0 min	53.5	29.9	0.0	16.6	$Ba_{0.5}Sr_{0.5}CO_3$
Ba50-Sr50 0 min	0.0	17.9	19.5	62.6	$Ba_{0.5}Sr_{0.5}TiO_3$
Ba20-Sr80 0 min	18.8	4.0	39.7	37.5	$Ba_{0.25}Sr_{0.75}TiO_3$

Rietveld analysis of pre-sintered samples (Tab. I) shows that the chemical reaction of formation of $Ba_xSr_{1-x}TiO_3$ can occur immediately after the mixing of powders, in samples with higher Sr content, and is most prominent in the sample with 50% Sr, where around 63 wt.% of $Ba_xSr_{1-x}TiO_3$ phase was observed. In the sample with 20% Sr, the dominant phase is anatase $TiO_2$with around 53 wt.%. The appearance of $Ba_xSr_{1-x}TiO_3$ phases in the samples suggests that the formation of $Ba_xSr_{1-x}TiO_3$ phases occurs relatively easily and well below sintering temperature, and therefore it is most likely completed before the onset of the sintering process. Formation of $Ba_{0.5}Sr_{0.5}CO_3$ highlights the ease with which Ba and Sr are interchangeable in the lattice, thus allowing the easy formation of mixed compounds.

Tab.II Microstructural parameters for newly formed phases in pre-sintered samples.

Sample	Phase	Lattice parameters (Å)	Average crystallite size (nm)	Microstrain	wt.%
Ba80-Sr20 0 min	$Ba_{0.5}Sr_{0.5}CO_3$	5.3002 ± 0.0001 6.4245 ± 0.0001 8.9064 ± 0.0001	60 ± 10	0.36± 0.03	16.6
Ba50-Sr50 0 min	$Ba_{0.5}Sr_{0.5}TiO_3$	3.9556 ± 0.0001	120 ± 10	0.27 ± 0.03	62.6
Ba20-Sr80 0 min	$Ba_{0.25}Sr_{0.75}TiO_3$	3.9066 ± 0.0001	110 ± 10	0.30 ± 0.04	37.5

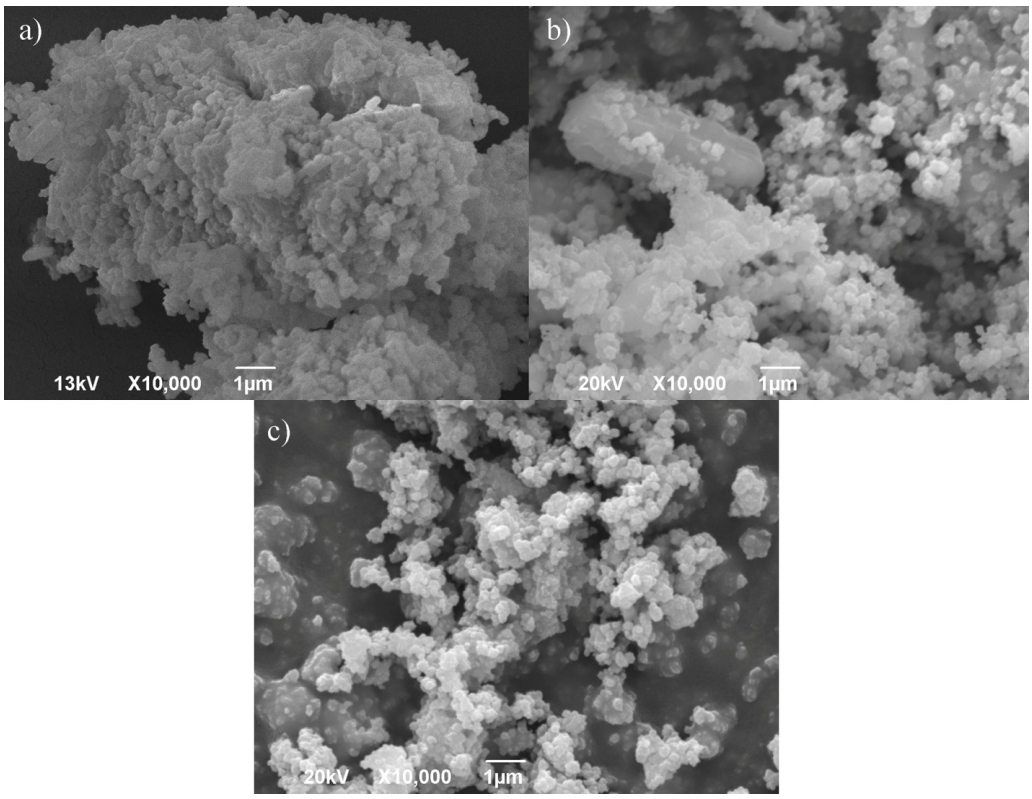

Fig. 2. SEM images for different Ba:Sr ratios: a) 80:20, b) 50:50 and c) 20:80.

SEM images in Fig. 2 show that composition of $Ba_xSr_{1-}xTiO_3$ powder has an effect on microstructure. Sample with 20% Sr exhibits a significantly higher degree of agglomeration

than the samples with other phase compositions and, in general, higher Sr content leads to larger particle size and less agglomerated samples, which is consistent with Rietveld analysis of XRD data.This can be attributed to the reaction between $BaCO_3$, $SrCO_3$ and TiO_2, where newly formed titanate phases most likely have narrower size distribution than the initial commercial powders.

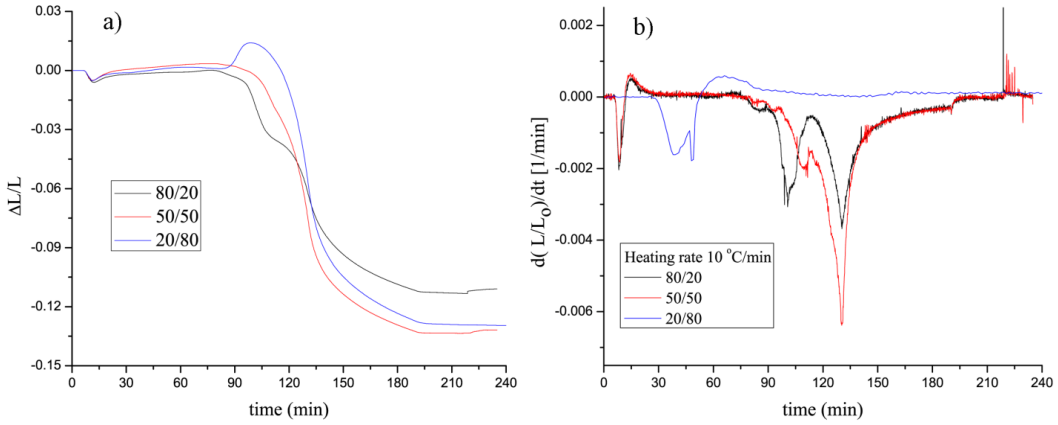

Fig. 3. Dilatometric measurements of samples with different Ba:Sr ratios at the heating rate of 10 °C/min.

Dilatometric measurements of samples with different Ba:Sr ratios shows that there are significant differences in the effect that sample composition has on the onset of sintering (Fig. 3a). For the samples with 20:80 Ba:Sr ratio, the onset of sintering overlaps with a process that causes expansion in the sample, causing the onset of shrinking to be shifted towards higher temperatures. Considering that, the formation of $Ba_xSr_{1-x}TiO_3$ phases should be completed well before the onset of sintering and according to the fact that the pre-sintered samples were heated at 800 °C to remove carbonates, the process resulting the expansion is most likely some phase transformation of $Ba_xSr_{1-x}TiO_3$ phase. The sample with 50:50 ratio exhibits higher temperature of the onset of sintering compared to the sample with 80:20 ratio, and no obviously visible phase transition, while the sample with 80:20 Ba:Sr ratio exhibits the lowest temperature of the onset of sintering and a clearly visible phase transition corresponding to the shoulder observed around 120 min in Fig. 3. The differential curves show the complexity of the sintering process, and the phase transition can be observed more clearly here (Fig. 3b). It is clear that the phase transition occurs in all three samples with different compositions, however, it appears to be more spread out in the sample with 50:50 ratio and sharper and well defined in samples with 80% of either Ba or Sr. It is also clear that the phase transition temperature decreases with increase in Sr content. $BaTiO_3$ exhibits a high-temperature phase transition from cubic to hexagonal phase around 1450°C, which can be lowered to around 1100 °C by addition of additives like $MnCO_3$ [39]. In this case, it is possible that the presence of Sr decreases the phase transition temperature leading to the observed expansion in the sample. The observed phase transition temperature is around 1150 °C in the sample with 80% Ba, which is lowered to around 900 °C for the sample with 80% Sr (Fig. 4a). This is consistent with lower temperature value for the cubic-to-tetragonal phase transition in $SrTiO_3$ as well as $(Ba,Sr)TiO_3$, compared to the temperature in $BaTiO_3$ [40]. In addition, it also likely that the temperature of the phase transition is reduced by the relatively small crystal size of the initial powder because of the previously sintered sample with 80:20 Ba:Sr ratio exhibits no visible phase transition up to 1300 °C. Since sintered samples are typically micro-rather than nano-sized [41], this would suggest that there is a strong size-

related effect on the hexagonal-to-cubic phase transition temperature of $Ba_xSr_{1-x}TiO_3$ phases. This would be consistent with the behavior of $BaTiO_3$, where cubic-to-tetragonal phase transition exhibits size dependence in nanoparticles smaller than 100 nm [42].

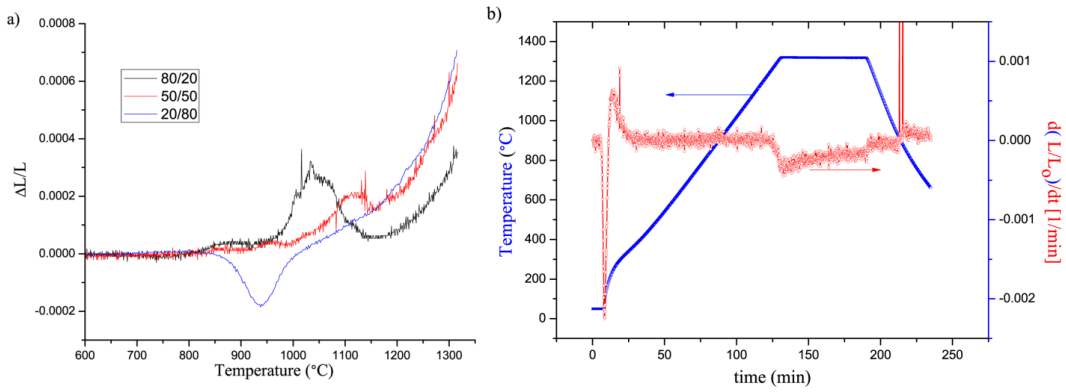

Fig. 4. Shrinkage rate as a function of the temperature of samples with different Ba:Sr ratios (left); dilatometric measurement of a previously sintered sample with Ba:Sr ratio of 80:20 (right).

Kinetic analysis of two segments of the dilatometric curve that correspond to the shrinking in the sample, on either side of the observed phase transition, is shown in Tab. III. It shows that the overall average value of activation energy and the average values of activation energy in the two segments follow the same trend with respect to the sample composition: they are the smallest for the sample with Ba:Sr ratio of 50:50 and larger in the other two, with sample with Ba:Sr ratio of 80:20 exhibiting the highest values of activation energy.This can be correlated with the fact that formation of $Ba_xSr_{1-x}TiO_3$ phase has occurred most readily in the sample with 50:50 ratio, where it would be relatively easy to achieve a homogeneous distribution of both Ba and Sr, creating favorable conditions for chemical reaction and sintering.

Tab.III Activation energies for BST powders determined using Wang-Raj method [43, 44].

Temp. Region (K)	**Ba20 – Sr80 (KJ/mol)**	**Ba50 – Sr50 (KJ/mol)**	**Ba80 – Sr20 (KJ/mol)**
Overall average	298	251	301
1300-1500	186	137	209
1500-1600	312	292	351

The second temperature segment exhibits significantly higher values of the apparent activation energy, what can be correlated with both the observed phase transition and densification of the sample as the result of sintering. This is especially obvious in the sample with 50:50 ratio, suggesting that the phase transition significantly compensates the effects of microstructure and chemical composition of the initial powder, otherwise present on the sintering process diagrams.

4. Conclusion

Sintering properties of barium strontium titanate (BST) system were investigated over a range of different Ba:Sr ratios. A mixture of $BaCO_3$, $SrCO_3$ and $TiO_2$was shown to react during the mixing and homogenization of powders to produce $Ba_{0.5}Sr_{0.5}CO_3$ or $Ba_{1-x}Sr_xTiO_3$, depending on Ba:Sr ratio. Equal parts of Ba and Sr appear to combine more easily since this mixture exhibited the highest content of $Ba_{1-x}Sr_xTiO_3$ phase on mixing as well as the lowest values of average apparent activation energy during sintering. While the temperature of the onset of sintering shifts to higher temperatures with an increase in Sr-content, the temperature position of the observed phase transition is, a contrary, lower in Sr-rich sample. The behavior of the phase transition is consistent with low-temperature phase transitions in BST, and its disappearance in sintered samples suggests also powder particle size-dependence of the phase transition temperature – something that has previously been observed in phase transitions in $BaTiO_3$.

Acknowledgments

These studies were performed in the project framework of OI 172057, financed by The Ministry of Education and Science of Republic of Serbia projects F/198, funded by Serbian Academy of Science and Arts.

5. References

1. A. M. Glazer, The classification of tilted octahedra in perovskites, Acta Crystallogr., Sect. B: Struct. Crystallogr. Cryst. Chem., 28 (1972) 3384-3392.
2. A. M. Glazer, Simple ways of determining perovskite structures, Acta Cryst, A31 (1975) 756-762.
3. S. Fuentes,R. Zárate,E. Chávez, P. Muñoz, D. Díaz-Droguett, Preparation of $SrTiO_3$ nanomaterial by sol-gel hydrothermal method, Journal of Material Science, 45 (2010) 1448-1452.
4. N. Labus, Z. Z. Vasiljević, D. Vasiljević-Radović, S. Rakić, M. V. Nikolić, Two Step Sintering of $ZnTiO_3$ Nanopowder, Sci. Sinter., 49 (2017) 51-60.
5. A. R. Đorđević, D. I. Olćan, N. Obradović, V. Paunović, S. Filipović, V. B. Pavlović, Electrical Properties of Magnesium TitanateCeramics Post-Sintered by Hot Isostatic Pressing, Sci. Sintering, 49 (2017) 373-380.
6. J. W. Liou, B. S. Chiou, Dielectric characteristics of doped $Ba_{1-x}Sr_xTiO_3$ a the paraelectric state, Mater. Chem. Phys., 51 (1997) 59-63.
7. K. Takemura, T. Sakuma, Y. Miyasaka, High dielectric constant (Ba,Sr)TiO_3 thin films prepared on RuO_2/sapphire, Appl. Phys. Lett., 64 (1994) 2967-2969.
8. T. Kawahara, M. Yamamuka, A. Yuuki, K. Ono, Surface morphologies and electrical properties of (Ba,Sr)TiO_3 films prepared by two-step deposition of liquid source chemical vapor deposition, Jpn. J. Appl. Phys., 34 (1995) 5077-5082.
9. S. Ezhilvalavan, T. Y. Tseng, Progress in the developments of (Ba,Sr) TiO_3 (BST) thin films for Gigabit era DRAMs, Mater. Chem. Phys., 65 (2000) 227-248.
10. L. Wu, Y. C. Chen, L. J. Chen, Y. P. Chou, Y. T. Tsai, Preparation and microwave characterization of $Ba_xSr_{1-x}TiO_3$ ceramics, Jpn. J. Appl. Phys., 38 (1999) 5612-5615.
11. T. Aoyama, S. Yamazaki, K. Imai, Characteristics of (Ba,Sr)TiO_3 capacitors with textured Ru bottom electrode, Jpn. J. Appl. Phys., 39 (2000) 6348-6357.

12. S. S. Lim, M. S. Han, S. R. Hahn, S. G. Lee, Dielectric and pyroelectric properties of (Ba,Sr,Ca)TiO_3 ceramics for uncooled infrared detectors, Jpn. J. Appl. Phys., 39 (2000) 4835-4838.
13. H. Y. Chang, K. S. Liu, I. N. Lin, Modification of PTCR behavior of $(Sr_{0.2}Ba_{0.8})TiO_3$ materials by post-heat treatment after microwave sintering, J. Eur. Ceram. Soc., 16 (1996) 63-70.
14. Y. J. Wu, Y. H. Huang, N. Wang, J. Li, M. S. Fu, X. M. Chen,Effects of phase constitution and microstructure on energy storage properties of barium strontium titanate ceramics, Journal of the European Ceramic Society, 37 (2017) 2099-2104.
15. D. Czekaj, A. Lisińska-Czekaj, T. Orkisz, J. Orkisz, G. Smalarz, Impedance spectroscopic studies of sol-gel derived barium strontium titanate thin films, Journal of the European Ceramic Society, 30 (2010) 465-470.
16. R. Schafranek, A. Giere, A. G. Balogh, T. Enz, Y. Zheng, P. Scheele, R. Jakoby, A. Klein,Influence of sputter deposition parameters on the properties of tunable barium strontium titanate thin films for microwave applications, Journal of the European Ceramic Society, 29 (2009) 1433-1442.
17. A. K. Tagantsev, V. O. Sherman, K. F. Astafiev, J. Venkatesh, N. Setter, Ferroelectric materials for microwave tunable applications, J. Electroceram., 11 (2003) 5-66.
18. P. Yu, B. Cui, Q. Shi, Preparation and characterization of $BaTiO_3$ powders and ceramics by sol-gel process using oleic acid as surfactant, Mater. Sci. Eng. A, 473 (2008) 34-41.
19. J. W. Liou, B. S. Chiou, Dielectric characteristics of doped $Ba_{1-x}Sr_xTiO_3$ at the paraelectric state, Mater. Chem. Phys., 51 (1997) 59-63.
20. Nisha D. Patel, M. H. Mangrola, Krishna G. Soni, V. G. Joshi, Structural and Electrical Properties of Nanocrystalline Barium Strontium Titanate, Materials Today: Proceedings 4 (2017) 3842-3851.
21. S. Fuentes, E. Chávez, L. Padilla-Campos, D. E. Diaz-Droguett, Influence of reactant type on the Sr in corporation grade and structural characteristics of $Ba_{1-x}Sr_xTiO_3$ (x=0-1) grown by sol–gel-hydrothermal synthesis, Ceramics International, 39 (2013) 8823-8831.
22. D. Hennings, Review of chemical preparation routes for barium titanate, Br. Ceram. Proc., 41 (1989) 1-10.
23. P. Pinceloup, C. Courtois, A. Leriche, B. Thierry, Hydrothermal synthesis of nanometer-sized barium titanate powders: control of barium/titanium ratio, sintering, and dielectric properties, J. Am. Ceram. Soc., 82 (1999) 3049-3056.
24. V. Kumar, Solution-precipitation of fine powders of barium titanate and strontium titanate, J. Am. Ceram. Soc., 82 (1999) 2580-2584.
25. B. A Wechsler, K. W. Kirby, Phase equilibria in the system barium titanate–strontium titanate, J. Am. Ceram. Soc., 75 (1992) 981.
26. T. Noh, S. Kim, C. Lee, Chemical preparation of barium– strontium-titanate, Bull. Korean Chem. Soc., 16 (1995) 1180.
27. D. Bao, Z. Wang, W. Ren, L. Zhang, X. Yao, Crystallization kinetics of $Ba_{0.8}Sr_{0.2}TiO_3$ sols and sol-gel synthesis of $Ba_{0.8}Sr_{0.2}TiO_3$ thin films, Ceramics International, 25 (1999) 261.
28. D. Dong, X. Liu, H. Yu, W. Hu, Fabrication of highly dispersed crystallized nanoparticles of barium strontium titanate in the presence of N,N-dimethylacetamide, Ceramics International, 37 (2011) 579-583.
29. Ghosh, D.,Tunable Microwave Devices Using BST (Barium Strontium Titanate) and Base Metal Electrodes, Graduate Faculty of the North Carolina State University, 2005. http://repository.lib.ncsu.edu/ir/handle/1840.16/4265.
30. Mason, W., Electrostrictive effect in barium titanate ceramics, Physical Review 74, No. 9 (1948) 1134-1147.

31. J. W. Liou, B. S. Chiou, Analysis of the dielectric characteristics for polycrystalline $Ba_{0.65}Sr_{0.35}TiO_3$ (I)-frequency dependence in the paraelectric state, J. Mater. Sci. Mater. Electron., 11 (2000) 637-644.
32. S. M. Olhero, A. Kaushal, J. M. F. Ferreira, Fabrication of Barium Strontium Titanate ($Ba_{0.6}Sr_{0.4}TiO_3$) 3D Microcomponents from Aqueous Suspensions, J. Am. Ceram. Soc., 97 (2014) 725-732
33. J. Wang, X. Yao, L. Zhang, Preparation and dielectric properties of barium strontium titanate glass-ceramics sintered from sol–gel-derived powders, Ceramics International, 30 (2004) 1749-1752.
34. D. Kosanović, N. Obradović, J. Živojinović, A. Maričić, V. P. Pavlović, V. B. Pavlović, M. M. Ristić, The Influence of Mechanical Activation on Sintering Process of $BaCO_3$-$SrCO_3$-TiO_2 System, Science of Sintering, 44 (2012) 271-280.
35. D. Kosanović, N. Obradović, J. Živojinović, S. Filipović, A. Maričić, V. Pavlović, Y. Tang, M. M. Ristić, Mechanical-Chemical Synthesis $Ba_{0.77}Sr_{0.23}TiO_3$, Science of Sintering, 44 (2012) 47-55.
36. D. Kosanović, J. Živojinović, N. Obradović, V. P. Pavlović, V. B. Pavlović, A. Peleš, M. M. Ristić, The influence of mechanical activation on the electrical properties of $Ba_{0.77}Sr_{0.23}TiO_3$ ceramics, Ceramics International, 40 (2014) 11883-11888.
37. B. H. Toby, R. B. Von Dreele, GSAS-II: the genesis of a modern open-source all purpose crystallography software package, J. Appl. Crystallogr., 46 (2013) 544-549.
38. J. M. Cork, S. L. Gerhard, Crystal Structure of the Series of Barium and Strontium Carbonates, Am. Mineral., (1931) 71.
39. R. M. Glaister, H. F. Kay, An Investigation of the Cubic-Hexagonal Transition in Barium Titanate, Proc. Phys. Soc. 76 (1960) 763-771.
40. H. Frayssignes, B. L. Cheng, G. Fantozzi, T.W. Button, Phase transformation in BST ceramics investigated by internal friction measurements, Journal of the European Ceramic Society, 25 (2005) 3203-3206.
41. N. Labus, S. Mentus, S. Rakić, Z. Z. Đurić, J. Vujančević, M. V. Nikolić, Reheating of Zinc-titanate Sintered Specimens, Science of Sintering, 47 (2015) 71-81.
42. M. B. Smith, K. Page, T. Siegrist, P. L. Redmond, E. C. Walter, R. Seshadri, L. E. Brus, M. L. Steigerwald, Crystal structure and the paraelectric-to-ferroelectric phase transition of nanoscale $BaTiO_3$, J. Am Chem Soc.,130 (2008) 6955-6963.
43. J. Wang, R. Raj, Estimate of the Activation Energies for Boundary Diffusion from Rate-Controlled Sintering of Pure Alumina, and Alumina Doped with Zirconia or Titania, J. Am. Ceram. Soc., 73(5) (1990) 1172-1175.
44. J. Wang, R. Raj, Activation Energy for the Sintering of Two-Phase Alumina/Zirconia Ceramics, J. Am. Ceram. Soc., 74(8) (1991) 1959-1963.

Садржај: *Прахови баријум стронцијум титаната различитих односа Ba:Sr су испитивани ради утврђивања утицаја почетног састава смеше на микроструктурна својства и кинетику синтеровања. Утврђено је даBaCO₃ и SrCO₃ различито реагују пре мешању, па је производ смеше са 80% Ba $Ba_{0.5}Sr_{0.5}CO_3$ и различите фазе $Ba_{1-x}Sr_xTiO_3$ у узорцима са 50% и 20% Ba. Такође, долази до промене морфологије, где већи садржај Sr води већој величини честица и мањем степену агломерације. Различит хемијски састав почетне смеше такође има значајан утицај на процес синтеровања: пошетак синтеровања се помера ка вишим температурама са повећањем удела Sr, док је просечна енергија активације синтеровања највиша у узорку са 80% Ba, а најнижа у узорку са 50% Ba. Фазни прелаз из хексагоналне у кубичну фазу се дешава паралелно са процесом синтеровања и температура овог прелаза се помера ка нижим температурама са повећањем удела Sr у узорку.Ово је у складу са понашањем ниско-*

температурског фазног прелаза у баријум стронцијум титанату. Фазни прелаз није уочен у синтерованим узорцима, што указује да постоји зависност температуре фазног прелаза од величине кристалита.
Кључне речи: *Баријум стронцијум титанат; Кинетика синтеровања; Фазни прелаз; зависност од величине.*